

Structure and Defects in Sanidic Liquid Crystalline Polymers. 1

I. G. Voigt-Martin* and P. Simon

Institut für Physikalische Chemie der Universität Mainz, Jakob Welder Weg 11, 55099 Mainz, Germany

S. Bauer and H. Ringsdorf

Institut für Organische Chemie der Universität Mainz, Becher Weg 18-20, 55099 Mainz, Germany

Received May 2, 1994; Revised Manuscript Received July 22, 1994*

ABSTRACT: A series of polymeric "sanidic" materials were investigated and a number of criteria developed which must be fulfilled in order to classify these materials as liquid crystalline. By a combination of electron diffraction and high-resolution imaging, the biaxial phase is shown to consist of poorly developed microcrystals embedded in a liquid-like amorphous matrix. Only some materials are able to form a liquid crystalline phase at higher temperatures, but this phase is uniaxial.

I. Introduction

Sanidic, or "boardlike", liquid crystals are fully aromatic polymeric amides/esters/enamines with alkyl side chains. Mesogenic groups consisting of low molecular weight rodlike polyamides have been known for a long time,¹ but real progress was not made until higher molecular weight materials were synthesized.² These stiff molecules have lyotropic liquid crystalline properties in solution and can be spun to form high-strength fibers. Unfortunately, the unsubstituted polyesters/amides are insoluble and tend to degrade before melting.

To alleviate this problem, flexible spacers³ or kinks⁴ can be introduced into the main chain. An alternative route to better solubility is the introduction of alkyl side chains.

Both low level substituted polymers⁵⁻¹¹ and highly substituted systems^{11,12} have been investigated by X-ray diffraction and deuterium NMR methods. Several structural models were proposed (Figure 1a-c) by these groups. The molecular origin of the observed long spacings and the role of the alkyl chains in controlling the packing of these systems are still not completely understood.

The investigations described in the following were undertaken in order to make a contribution toward understanding the role of the main chain and the alkyl side chains in controlling molecular ordering in these materials. Some fundamental problems concerning the interpretation of the scattering patterns are described in the following:

The characteristic X-ray and electron diffraction patterns are comprised of two perpendicular series of diffraction maxima in the small-angle and wide-angle regions (biaxial order) in addition to a broad halo in the wide-angle region. After the first investigations, a problem arose in connection with these diffraction patterns; namely, are they characteristic of a liquid crystalline mesophase at all or simply a poorly developed crystalline phase? The textures observed in these highly viscous materials by light microscopy were not typical of any known liquid crystalline phase, and the DSC diagrams did not show any evidence enabling a clear decision to be made as to whether transitions between crystalline or liquid crystalline mesophases

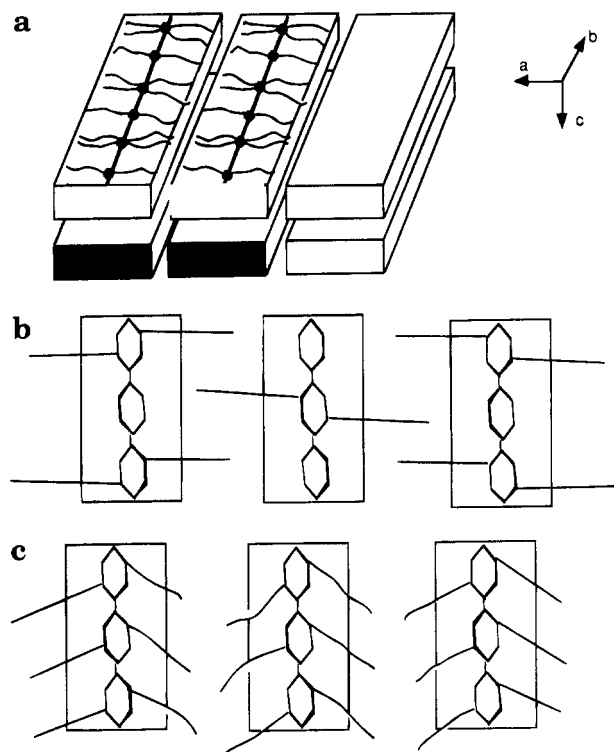


Figure 1. (a) Boardlike structure of highly substituted sanidic liquid crystalline polymers. (b) Model of low level substituted main chain polymer with interdigitated alkyl chains. (c) Scheme of arrangement of polyamide with four alkyl chains per repeat unit.

were responsible for the enthalpies obtained. In addition to this, the biaxial diffraction patterns give rise to maxima which can also be related to a poorly developed crystalline phase. The samples with the best orientation produced fiber diffraction patterns with a wide orientational distribution which can be simulated using a paracrystalline model structure.

For this reason it became mandatory to develop criteria which can enable a distinction to be made between a biaxial liquid crystal in the glass phase and a poorly developed semi-"crystalline" polymer in an amorphous matrix. In addition, it is important to understand the conditions under which such a distinction is no longer possible using structural methods, which give only static correlation functions. The strategy developed in this work was therefore as follows:

* Abstract published in *Advance ACS Abstracts*, November 15, 1994.

1. Differential scanning calometry was used to observe the behavior of individual enthalpic peaks on a series of samples using different heating rates.

2. Electron diffraction patterns were recorded in specific temperature intervals below and above the transition temperatures. Three features were investigated: (a) The value of the small-angle long spacing L and the perpendicular wide-angle spacing w , (b) the profile of the scattering maximum and its full width at half-maximum (fwhm), and (c) the contour shape of the small-angle spacing.

3. High-resolution electron microscopy was used to determine the shape and distribution of the scattering regions as well as to examine the nature of their defects.

4. Detailed information about the molecular ordering was obtained by electron diffraction from monomeric analogs (Part 2). Important information about the polymer can be induced from the results.

II. Methods of Investigation

1. Electron Diffraction. Structural analysis has made tremendous progress in recent years because powerful techniques like direct phase methods,¹⁴ maximum entropy statistics,¹⁵⁻¹⁷ and computer simulations of experimental diffraction patterns¹⁸ can now be applied successfully using electron diffraction. This means that the structure of very small organic microcrystals can be resolved to give molecular resolution. However, all structural analysis methods require a large number of reflections and rely on symmetry relations for space group determination. These two criteria are not satisfied by liquid crystals. To alleviate this problem, monomeric analogs can be crystallized and heated into the liquid crystalline phase. The changing diffraction pattern is monitored throughout the process, and generally it is then possible to correlate molecular dimensions and orientation before and after the transition with the observed diffraction pattern.¹⁹ This procedure has also been adopted in this work. The simulation of the diffraction patterns from monomeric analogs will be described in Part 2 (following paper in this issue), and it will be shown that this gives vital information regarding the structure of the liquid crystalline phase.

The characteristic difference between the electron diffraction from a crystal and a liquid crystal is described in the following:

An electron diffraction pattern from a crystal with three-dimensional order is a two-dimensional projection and should give intensities and extinctions corresponding to 1 of the 17 plane groups.²⁰ By appropriate tilting, other projections can be obtained and the three-dimensional crystal analyzed, in which case the space group can be determined. If translational correlations are infinite, the peaks are δ functions. Frequently, however, crystal defects lead to spot broadening, so that the intensity profile can be described by a Gaussian distribution (dislocations) or Lorentzian distribution (paracrystalline disorder). In the kinematical case, any systematic absences related to symmetry elements should be retained, although there are exceptions to this rule.^{21,22} If there are defects or if the crystal thickness increases, higher order reflections are lost. Dynamical diffraction effects may cause forbidden reflections to appear.

The electron diffraction pattern from a liquid crystal, however, has to be considered in terms of the correlation function $g_2(r)$ describing the molecular positions in real space. This correlation function can be obtained from

its Fourier transform, the scattering function $s(q)$. In layer-like liquid crystals, $s(q)$ consists of a series of very sharp peaks (δ functions) with an algebraic decay only in the wings of the intensity maximum.²³ This can be related to the elastic constants in smectic liquid crystals. We have shown in previous investigations on smectic and discotic systems that this applies not only to monomeric but also to polymeric liquid crystals.^{18,24,25}

However, in liquid crystals there should not be any symmetry-induced absences, since symmetry is broken in the liquid crystalline mesophase. In thick biaxial samples with many different types of defects, the distinction between a liquid crystal and a crystal becomes quite difficult, but symmetry-related systematic absences, which should not occur in liquid crystals, are a strong indication for crystalline-type order.

2. High-Resolution Imaging. In the previous section we have discussed some criteria which might be used to distinguish between the diffraction pattern from a biaxial liquid crystal and that of a poorly developed crystal in a two-dimensional projection, and we have indicated that the distinction may not always be easy. Another criterion may be sought in the high-resolution images. Liquid crystals have specific defects,²⁶ which do not occur in crystals. These defects depend on the liquid crystalline phase in question and have been made amenable to electron microscopic inspection, using various different techniques.^{18,25,27-29}

Several etching and contrasting techniques have been developed to make these defects visible. The method used in this investigation is the one developed in this group several years ago, involving the use of a very untypical phase contrast transfer function in order to transfer spatial frequencies corresponding to the small angle spacings observed in the diffraction pattern.^{25,30} The correct contrast transfer function is achieved by controlling the objective lens using a computer attached to the electron microscope via a suitable CCD camera. The Fourier transform of the image immediately indicates when the correct defocus value has been adjusted.

In addition to giving information about defect structures, high-resolution images also give directly the shape and distribution of the scattering regions.

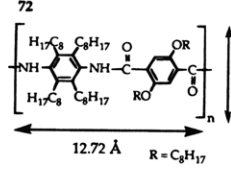
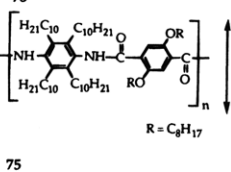
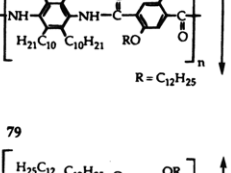
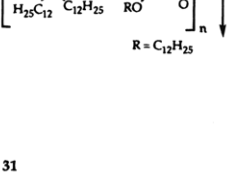
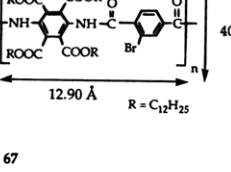
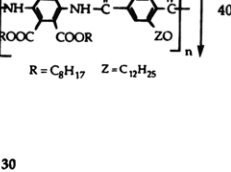
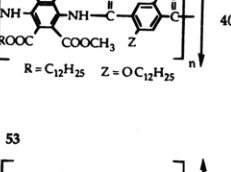
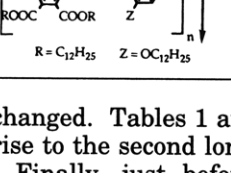
III. Results

1. Electron Diffraction. 1.1. Long Spacings. All the investigated samples produced a biaxial diffraction pattern below and above the glass transition temperature. In all cases the wide-angle maxima were related to twice the length of the monomeric main chain unit, which was between 24.8 and 25.6 Å long. Generally, the 5th- and 12th-order reflections were the most intense. The reason for the double length becomes clear only after detailed analysis of monomeric analogs (Part 2).

Perpendicular to these were a series of small-angle reflections. Their long spacing is related to the length of the side chains, but their value lies considerably below the length of the molecule with extended side chains, the difference being about 10 Å. The results are summarized in Tables 1 and 2. The small-angle reflections are not very sharp, an important feature which will be discussed in the following. They are labeled L_{cp} .

On raising the temperature, in some samples a second small but very sharp small-angle reflection L_s appeared, incommensurate with, but in the same direction as, the first and with a value corresponding to an even smaller long spacing. The wide-angle spacings remain un-

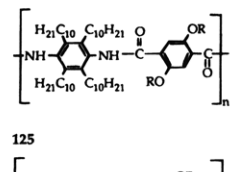
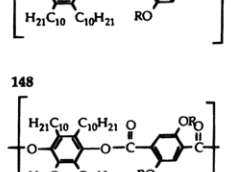
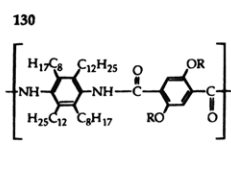
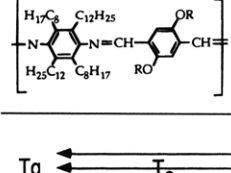
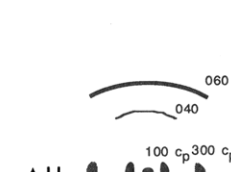
Table 1. Comparison of Sanidic Polymers with Different Side Chain Lengths

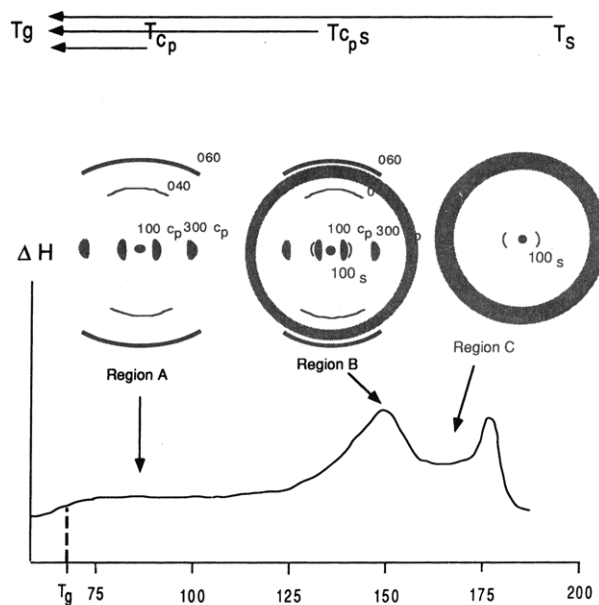
		Phase transition temperatures DSC (g = glass) (c = crystal) (i = isotropic)	Spacings obtained by electron diffraction $L_{cp} = L$ for paracrystal $L_s = L$ for liquid crystal
72		g/c 163 lc 208 i	$L_{cp} = 22.50 \text{ \AA}$ $w = 12.84 \text{ \AA}$ $L_s = 17.30 \text{ \AA}$
78		g 60 c 168 lc 180 i	$L_{cp} = 25.3 \text{ \AA}$ $w = 12.72 \text{ \AA}$ $L_s = 19.3 \text{ \AA}$
75		g 65 c 151 lc 183 i	$L_{cp} = 28.10 \text{ \AA}$ $w = 25.92 \text{ \AA}$ $d = 5.10 \text{ \AA}$ $L_s = 20.90 \text{ \AA}$
79		g/c 141 i	$L_{cp} = 25.20 \text{ \AA}$ $w = 12.57 \text{ \AA}$
31		g/c 270 decompos.	$L_{cp} = 28.37 \text{ \AA}$
67		g/c 51 lc 69 i	$L_{cp} = 19.85 \text{ \AA}$
30		g/c -17 lc 166 i	$L_{cp} = 22.5 \text{ \AA}$ $w = 13.0 \text{ \AA}$
53		g/c 17 c 67 lc 127 i	$L_{cp} = 28.5 \text{ \AA}$ $w = 12.9 \text{ \AA}$ $d = 7.8 \text{ \AA}$ $L_s = 24.0 \text{ \AA}$

changed. Tables 1 and 2 indicate which samples gave rise to the second long spacing L_s .

Finally, just before melting, the old small-angle spacing disappears and only the new, sharp reflection

Table 2. Comparison of Sanidic Polymers with Same Side Chain Length but Different Main Chains

		Phase transitions (DSC)	Molecule dimensions from electron diffraction
75		g 65 c 151 lc 183 i	$L_{cp} = 28.10 \text{ \AA}$ $w = 25.92 \text{ \AA}$ $d = 5.10 \text{ \AA}$
125		c1 55 c2 135 i	$L_{cp} = 29.50 \text{ \AA}$ $w = 25.46 \text{ \AA}$ $d = 5.10 \text{ \AA}$
148		g/c 89 i	$L_{cp} = 29.40 \text{ \AA}$ $w = 12.41 \text{ \AA}$ $d = 5.18 \text{ \AA}$
130		g 65 c 156 lc 180 i	$L_{cp} = 27.6 \text{ \AA}$
133		c1 25 c2 127 lc 200 i	$L_{cp} = 29.54 \text{ \AA}$ $w = 12.74 \text{ \AA}$ $d = 4.85 \text{ \AA}$

**Figure 2.** Schematic diagram showing the relationship between the thermal behavior and electron diffraction patterns obtained from sanidic samples at the temperatures indicated.

remains. The very weak wide-angle reflection perpendicular to it also disappears. These diffraction patterns are related to the DSC curves as indicated schematically in Figure 2.

Details regarding the relationship between the molecular length and the measured long spacings L for a series of molecules are given in Tables 1 and 2. In addition, the values of the wide-angle spacings w and d are listed. Their relations to the molecular structure are shown schematically in Figure 3. The phase transi-

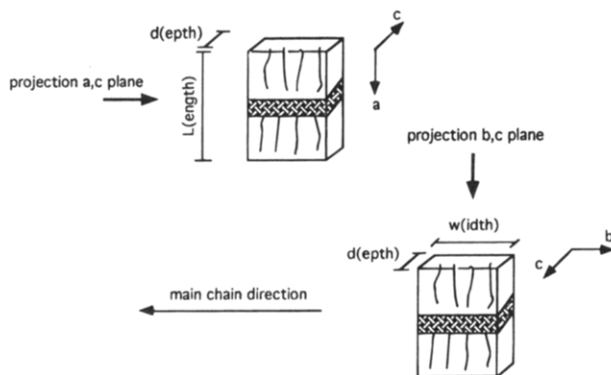


Figure 3. Molecular dimensions obtained from different projections.

tion temperatures are also given in Tables 1 and 2. Above T_g , several samples show two phase transitions. The value of L at the upper transition temperature is labeled L_s and at the lower transition temperature L_{cp} .

Careful investigation of the results shows that the length of the side chain is clearly correlated with the observed long spacing L in all three regions.

In the low-temperature phase therefore the layer distance is about 10 Å less than the length corresponding to the molecule with fully extended side chains, and in the high-temperature phase this is reduced by another 3–8 Å. Possible reasons for such a reduction could be intercalation of the side chains or tilting (see Figure 1). Both possibilities will be discussed in the following. However, as a first step toward understanding the molecular origins of the observed features, some specific peculiarities of the electron diffraction patterns must be discussed.

1.2. Nature of the Diffraction Pattern. Region

A. Region A of Figure 2 lies above the glass transition temperature, and the diffraction pattern from samples in this region is purely biaxial. There are no reflections having mixed indices in this zone. This suggests that the sample is in a liquid crystalline phase. However, there are some remarkable features in the diffraction pattern which are reminiscent of a crystal:

Of the wide-angle reflections and sometimes in the case of the small-angle reflections, there are missing orders, and frequently large-order reflections have higher intensities than smaller orders. This is typical of crystals with symmetry-related absences and intensities related to the structure factors of specific (hkl) reflections. Furthermore, the small-angle layer reflections in liquid crystals should be very sharp whereas these small-angle reflections in the biaxial phase are very broad. Numerical analysis shows that they are oval (Figure 4).

Unfortunately, the discussion about paracrystals has not always been carried out objectively. However, it has been shown by many groups that the scattering function from a disturbed crystal lattice having specific lattice statistics is described by a Lorentzian function. The criteria distinguishing the so-called ideal paracrystal from the physically possible Gaussian paracrystal or the disturbed layer lattice have been discussed in detail in the literature.^{31–34}

For the biaxial "sanidic" samples in question, the small-angle maximum corresponding to a value between 22 Å (sample 30) and 28 Å (sample 75) obtained by electron diffraction in region A is Lorentzian in the radial direction and its full width at half-maximum corresponds to a correlation length of 340 Å perpen-

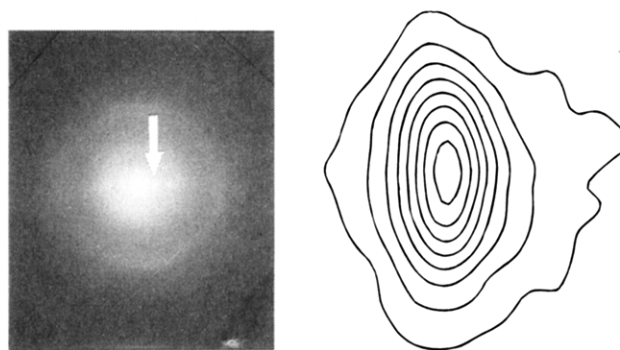


Figure 4. Electron diffraction pattern and contour plot of layer reflection of polyamide 30.

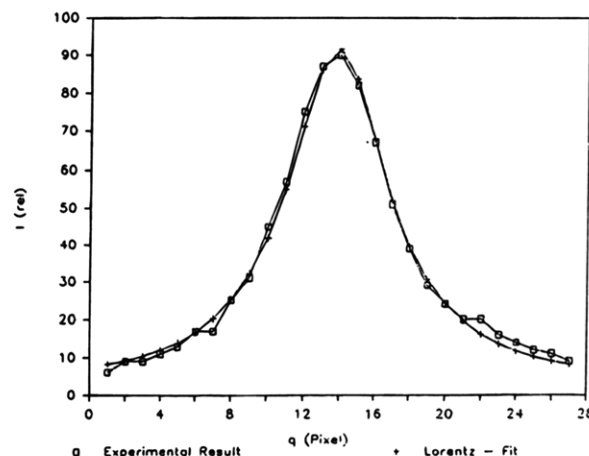


Figure 5. Radial plot of layer reflection of electron diffraction (Lorentzian) with fwhm of 0.003 Å (region A).

dicular to the layers (Figure 5). The line shape therefore does not correspond to the one expected for a liquid crystal and the correlation length is too small for quasi-long-range order.

Region B (Samples 72, 75, and 78). In this region the old small-angle spacing remains broad while a new, noncommensurate sharp reflection appears, corresponding to a value about 5 Å less than L_{cp} . The sample consists of several phases: (a) biaxial, (b) uniaxial, and (c) amorphous. The new phase is oriented in the same direction as the old one.

Region C (Samples 72, 75, and 78 only). Shortly before passing into the isotropic melt, the old small-angle reflection disappears and the new, sharp small-angle reflection appears with a full width at half-maximum corresponding to a correlation length of about 800 Å. This structure is unequivocally liquid crystalline and has been labeled as such in Table 1. The wide-angle reflections at 4.3 Å arising from the polymer backbone become weak and finally disappear in the LC phase. This indicates that the correlation between the side chains is strongly disturbed in a direction perpendicular to the layers. These observations fit well with experiments on low level substituted systems, where the wide-angle reflections also began to disappear in the LC phase.⁵

Amorphous Halo. Above the glass transition an amorphous halo is observed but most intensely in the liquid crystalline state. The halo is sometimes isotropic but occasionally shows some preferred orientation.

The amorphous halo could arise from structural fluctuations within a liquid crystalline phase, in which case region A could also be a liquid crystalline phase. However, it could also arise if crystals are distributed

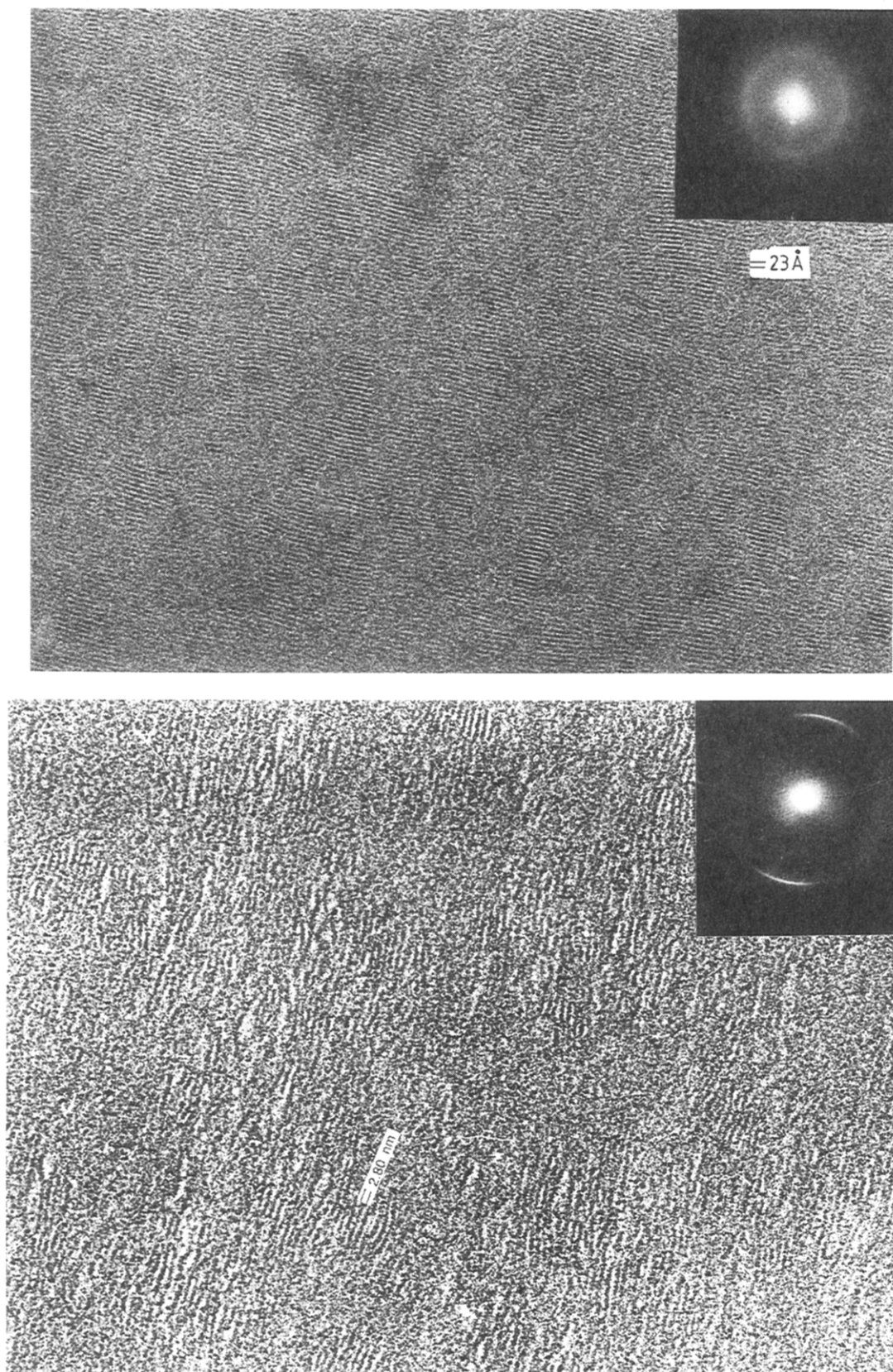


Figure 6. High-resolution image of polyamide 30 with electron diffraction pattern. High-resolution micrograph of "sanidic layers" of sanidic polymer 75 in the crystalline phase and corresponding electron diffraction pattern.

in an amorphous matrix. To distinguish between these possibilities, high-resolution images were obtained. In addition to this, the structure analysis of the monomers described in section II gives reliable information regarding the origin of the halo.

2. High-Resolution Imaging. High-resolution images can be obtained only from samples in the solid

state, in other words, below the glass transition. Therefore the images represent the structure of a quenched state (glass). Figure 6a and 6b show such images from two polyamides which were well oriented (polyamide 30) and badly oriented (polyamide 75). In both cases, the oriented regions consist of blocks in which the layers are slightly (polyamide 30) or strongly (polyamide 75)

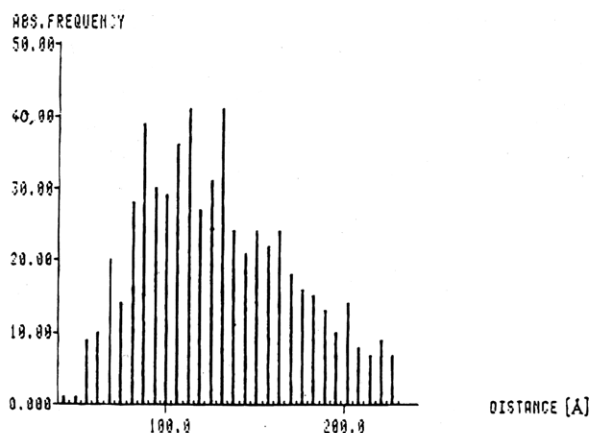


Figure 7. Distribution of M .

distorted and dislocations are sometimes observed. Between the blocks, there are regions without contrast. These must be responsible for the isotropic halo in the diffraction patterns. This information, which can only be obtained from images, is extremely important because it shows that the isotropic part of the amorphous halo in the biaxial phase is not related to a "liquid crystal" disorder but stems from these amorphous regions. At the same time the amorphous halo also indicated some preferential order, which must arise from disorder in the oriented regions. Finally, the molecular origin could only be determined from the simulations of diffraction patterns obtained from crystalline monomers as described in section II.

3. Numerical Analysis of Images. For the polyamide (sample 30) the size of the scattering regions was analyzed according to block width M (Figure 7) and block length G as well as the layer spacing L . The histograms show that block width M corresponds very well to the molecular length of the main chain (120 Å) of these samples, while the measured block length G gave an average value of about 300 Å. This value is only slightly larger than the correlation length deduced from the small-angle peak. In addition, the layer spacing within the blocks was 22 Å, corresponding to the small-angle spacing.

The relationship between the molecular structure and the diffraction pattern is therefore shown schematically in Figure 8.

Since the size of the oriented blocks is relatively limited, peak broadening is to be expected on this account. The orientational deviations observed in the high-resolution electron micrographs is slightly less than the arcing observed in the diffraction pattern ($\pm 15^\circ$). This is to be expected because the diffraction pattern is obtained from a much larger region.

However, the layer spacing L is considerably less than the length of the molecule with extended alkyl chains as already induced from the diffraction pattern. Their packing can be deduced only by analysis of the monomeric analogs, as described in Part 2.

4. Quenching Experiments. When the samples are quenched into the glassy phase from regions A, B, and C (Figure 2), the major features of the diffraction patterns remain unchanged, except for region C. In this case, the wide-angle reflections reappear, while the small-angle maximum remains sharp and retains the smaller long spacing L_s . This indicates that the orientation and long-range translational correlations are considerably improved by annealing in the liquid crystalline phase but that the oriented region tends to

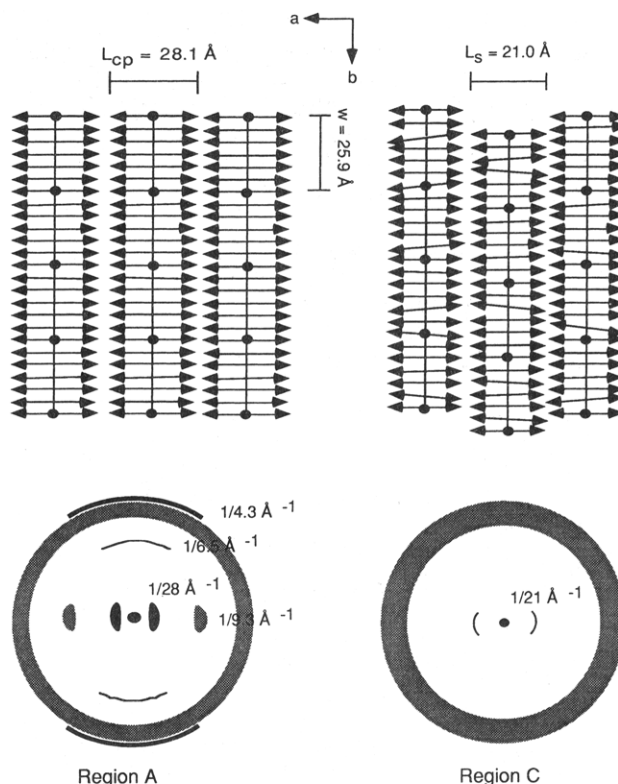


Figure 8. Relationship between molecular structure and electron diffraction patterns from regions A and C. Arrows indicate that L_{cp} and L_s are smaller than the distance corresponding to the extended side chain length.

recrystallize on quenching with the new long spacing L_s . The isotropic amorphous halo is a clear indication that these regions are embedded in a glassy amorphous matrix.

IV. Conclusion

The diffraction data obtained from sanidic polymers can only be understood if a series of samples are carefully chosen such that a specific parameter (length of side chain/main chain) is systematically varied and the line profiles as well as contour plots of the intensity maxima are analyzed numerically. Furthermore, the diffraction experiments were supplemented by high-resolution imaging in order to give crucial information regarding the cause of the broadening as well as about the distribution of scattering centers. Small blocks of oriented material are dispersed in an amorphous matrix. The layers within the blocks are distorted and reveal dislocations.

The analysis of these samples shows that the biaxial phase immediately above the glass transition consists of small, paracrystalline blocks embedded in an amorphous matrix. The reasons for defining these regions as paracrystalline are discussed in detail. They are related to the systematic absences in both wide- and small-angle reflections and to the broad, Lorentzian profile of the layer reflections. A further, even stronger argument will appear in Part 2, where monomeric analogs are analyzed. At a higher temperature, in some samples a new, much sharper, small-angle spacing appears, considerably more characteristic of a liquid crystalline phase. At the same time, the high-temperature phase is no longer truly biaxial but more reminiscent of a smectic phase but with motion restricted to one direction.

The analysis of a whole series of samples classified as "sanidic" has shown that only the amides are able to form a layered liquid crystalline phase, which is not, in fact, biaxial. Of the azomethines only sample 133 forms a liquid crystalline phase, but this was nematic.

The most important challenge remains that of ascertaining the precise reason for the 10–18 Å reduction in long spacing compared with the length L of the fully extended side chains. Any number of different models can be proposed to fit a sparse number of reflections. This problem has been solved in Part 2, by comparing the results obtained from crystalline monomeric analogs with one of these polymers.

References and Notes

- (1) Shashana, V. E.; Eriksen, W. E. *J. Polym. Sci.* **1959**, *11*, 343.
- (2) Morgan, P. W. *Condensation Polymers: By Interfacial and Solution Methods*; Interscience, New York, 1965 (*Polym. Rev.*, Vol. 10).
- (3) Jin, J. I.; Antoun, S.; Ober, C.; Lenz, R. W. *Br. Polym. J.* **1980**, *12*, 132.
- (4) Griffin, B. P.; Cox, H. K. *Br. Polym. J.* **1980**, *12*, 154.
- (5) Ballauff, M.; Schmidt, G. F. *Mol. Cryst. Liq. Cryst.* **1987**, *147*, 163.
- (6) Rodriguez-Parada, J. M.; Duran, R.; Wegner, G. *Macromolecules* **1989**, *22*, 2507.
- (7) Adam, A.; Spiess, H. W. *Makromol. Chem., Rapid Commun.* **1990**, *11*, 249.
- (8) Biswas, A.; Deutscher, K.; Blackwell, J.; Wegner, G. *Polym. Prepr. (Am. Chem. Soc., Div. Polym. Chem.)* **1992**, *33*, 286.
- (9) Yu, L.; Bao, Z.; Cai, R. *Angew. Chem.* **1993**, *105*, 1392.
- (10) Galda, P.; Kistner, D.; Martin, A.; Ballauff, M. *Macromolecules* **1993**, *26*, 1595.
- (11) Sone, M.; Harkness, I. B. R.; Watanabe, J.; Yamashita, T.; Torii, T.; Horie, K. *Polym. J.* **1993**, *25*, 997.
- (12) Ringsdorf, H.; Tschirner, P.; Herrmann-Schönherr, O.; Wendorff, J. H. *Makromol. Chem.* **1987**, *188*, 1431.
- (13) Ebert, M.; Herrmann-Schönherr, O.; Wendorff, J. H.; Ringsdorf, H.; Tschirner, P. *Liq. Cryst. Mol. Cryst.* **1990**, *7*, 63.
- (14) Dorset, D. *Ultramicroscopy* **1991**, *38*, 23.
- (15) Bricogne, G. *Acta Crystallogr.* **1984**, *A40*, 410.
- (16) Dong, W.; Baird, T.; Fryer, J. R.; Gilmore, C. J.; MacNicol, D. D.; Bricogne, G.; Smith, D. J.; O'Keefe, M. A.; Hovmöller, S. *Nature (London)* **1992**, *355*, 605.
- (17) Voigt-Martin, I. G.; Yan, D. H.; Gilmore, C. J.; Shankland, K. *Ultramicroscopy*, to be published.
- (18) Voigt-Martin, I. G.; Schumacher, M.; Garbella, R. W. *Macromolecules* **1992**, *25*, 961.
- (19) Voigt-Martin, I. G.; Schumacher, M.; Garbella, R. W. *Liq. Cryst.*, in press.
- (20) *International Tables of X-ray Crystallography*; Kynoch Press: Birmingham, England, 1959; Vol. 1.
- (21) Gijonnes, J. K.; Moodie, A. F. *Acta Crystallogr.* **1965**, *19*, 65.
- (22) Cowley, J. M. *Diffraction Physics*; North-Holland: Amsterdam, The Netherlands, 1984.
- (23) Als-Nielsen, J.; Litser, J. D.; Birgenau, R. J.; Kaglaur, M.; Sufuya, C. R.; Lindegard-Andersen, A.; Marthesen, S. *Phys. Rev.* **1980**, *B22*, 312.
- (24) Voigt-Martin, I. G.; Durst, H. *Macromolecules* **1989**, *22*, 168.
- (25) Voigt-Martin, I. G.; Krug, H.; Van Dyck, D. *J. Phys.* **1990**, *51*, 2347.
- (26) Demus, K.; Richter, L. *Textures in Liquid Crystals*; Verlag Chemie: Weinheim, 1978.
- (27) Thomas, E.; Wood, E. L. *Faraday Discuss. Chem. Soc.* **1985**, *79*, 229.
- (28) Voigt-Martin, I. G.; Durst, H. *Macromolecules* **1989**, *22*, 168.
- (29) Voigt-Martin, I. G.; Garbella, R. W.; Vallerien, S. U. *J. Phys.* **1991**, *2*, 345.
- (30) Voigt-Martin, I. G.; Durst, H. *Liq. Cryst.* **1987**, *2*, 601.
- (31) Bonart, R. *Kolloid Z. Z. Polym.* **1964**, *194*, 97.
- (32) Schönfeld, A.; Wilke, W.; Höhne, G.; Hoseman, R. *Kolloid Z. Z. Polym.* **1972**, *250*, 102.
- (33) Wilke, W. *Colloid Polym. Sci.* **1981**, *259*, 577.
- (34) Ruland, W. *Prog. Colloid Polym. Sci.* **1975**, *57*, 192.

MA940796K